PHYSICAL REVIEW VOLUME 141, NUMBER 3 JANUARY 1966

Isotopic Masses of Hydrogen, Chlorine, Barium, Cerium, and Neodymium*

JAY L. BENSON† AND WALTER H. JOHNSON, JR.
School of Physics and Astronomy, University of Minnesota, Minneapolis, Minnesota

(Received 30 August 1965)

The 16-in. double-focusing mass spectrometer at the University of Minnesota has been employed to measure the atomic mass of H^1 and the atomic masses and isotopic mass differences of chlorine, barium, cerium, and neodymium. Recent improvements in instrumentation have increased the precision of both narrow and wide doublet measurements. The doublet $C_{11}H_{22}-C_{12}H_{10}$ was used to relate the H^1 mass directly to the C^{12} mass standard with a precision of ±30 eV. The chlorine masses obtained in this investigation have a precision greater than previous measurements and provide further information about disagreements which were present in previous work. Additional atomic masses are calculated from the stable-mass data of barium, cerium, and neodymium, together with alpha-decay, beta-decay, and nuclear-reaction energies. The resultant table of masses is used to calculate nuclear systematic energies in the region near $N=82$. The systematics of the separation energies display very smooth characteristics except at the shell closure of $N=82$ and are so regular as to be a powerful aid in the evaluation of some possible errors in reaction and decay data used in the calculation of these nuclear systematics.

INTRODUCTION

PRECISE spectrometric atomic masses and mass differences are useful for the important role they have in the study of nuclear structure. In certain cases they also serve as an independent check on nuclear-reaction Q values. Over the past ten years the 16-in. double-focusing mass spectrometer at the University of Minnesota has been used for a rather systematic set of measurements of most of the stable isotopes from carbon to xenon.[1–7] Much of this previous work made use of narrow-doublet mass measurements, usually involving hydrocarbon comparison masses. Improvements in instrumentation have recently made possible the measurement of wider mass doublets, in particular single and double isotopic mass differences, with precision comparable to or better than that of the previous narrow-doublet technique. This wide-doublet technique has been tested and used in the present work for the measurement of the atomic masses and isotopic mass differences of the stable isotopes of barium, cerium, and neodymium. Nuclear-reaction and decay data have been combined with these measurements for a study of the nuclear systematics in this mass region.

Since hydrocarbon molecular or fragment ions are most often used as secondary mass standards in doublet mass measurements, it is important to have an accurate value for the hydrogen mass. Previous measurements of the hydrogen mass have been made under the O^{16} mass standard and have involved groups of interrelated doublet measurements. Under the new C^{12} mass standard it is possible to measure hydrogen versus the C^{12} standard directly. The result of a precise measurement of the mass of hydrogen is reported in this work. Because of inconsistencies in previous measurements, the chlorine isotopic masses and the isotopic mass difference were also measured.

THE INSTRUMENT

The basic instrument employed for all previous measurements has been described in detail elsewhere.[6,8,9] Doublets are measured by a peak-matching method in which the precision of a measurement depends upon three factors. First, the width of a mass peak wave form in mass units should be as small as practical. The resolution, defined as the mass of the particular ion divided by the width of the peak at one-half maximum, was between 90 000 and 125 000 for most of the presently reported work. Next, the precision of a measurement depends upon the ability of the operator to detect a mismatch of two mass peak wave forms such as shown in Fig. 1. In this figure the wave forms are mismatched by 10% of their width at half-height to more clearly

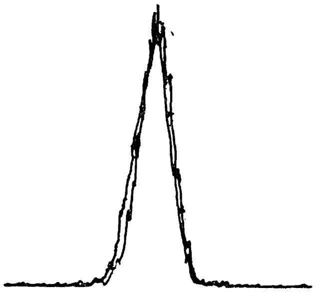

FIG. 1. A tracing of the mass peak wave forms of $(Ba^{136})^+$ ions and $(Ba^{137})^+$ ions presented on alternate sweeps of the magnetic field. The spectrometer fields are adjusted so that wave forms appear displaced by 10% of the width at half-maximum.

---

* Supported by Contract Nonr-710(58) with the U. S. Office of Naval Research.

† Present address: Sandia Corporation, Albuquerque, New Mexico.

[1] K. S. Quisenberry, T. T. Scolman, and A. O. Nier, Phys. Rev. **102**, 1071 (1956).

[2] T. T. Scolman, K. S. Quisenberry, and A. O. Nier, Phys. Rev. **102**, 1076 (1956).

[3] K. S. Quisenberry, T. T. Scolman, and A. O. Nier, Phys. Rev. **104**, 461 (1956).

[4] K. S. Quisenberry, C. F. Giese, and J. L. Benson, Phys. Rev. **107**, 1664 (1957).

[5] Clayton F. Giese and Jay L. Benson, Phys. Rev. **110**, 712 (1958).

[6] Richard R. Ries, Richard A. Damerow, and Walter H. Johnson, Jr., Phys. Rev. **132**, 1662 (1963).

[7] Richard A. Damerow, Richard R. Ries, and Walter H. Johnson, Jr., Phys. Rev. **132**, 1673 (1963).

[8] H. Hintenberger, *Nuclear Masses and Their Determination* (Pergamon Press, Inc., London, 1957), Session VII, p. 185.

[9] E. G. Johnson and A. O. Nier, Phys. Rev. **91**, 10 (1953).

show the presence of two mass peaks. Finally, in order to calculate a mass difference, the calibration and calculation of spectrometer electric-field ratios necessary to produce the superposition of the wave forms must be known precisely.

Previous work has used a visual detection of peak-shape mismatch. The final precision of this peak-matching technique was very good, but since only a limited number of individual sweeps were employed in the matching decision, individual matching errors were much greater than the final quoted error of the average of many matches. Systematic errors might be present with sufficient magnitude to affect the final average, while being too small to be detected on one individual setting. A new technique of detecting peak mismatch to greater accuracy was desirable for the investigation of possible systematic effects as well as for the capability of higher precision in the measurement of mass differences. In the new technique a digitial memory oscilloscope[10,11] is employed to allow the operator to use more scans of the mass doublet and, in addition, to observe a definite error signal indicating a mismatch rather than attempting to observe an exact superposition of two peaks. This digital memory unit is a wave form averaging device consisting of a voltage digitizer feeding a 1024-channel magnetic core memory in which each channel corresponds to a definite time interval following the start of the main oscilloscope sweep. This unit also allows a continuous display of stored data on the readout oscilloscope. As in the previous visual method, the sweep times of the oscilloscope viewing individual sweeps, the oscilloscope displaying the memory content, and the time base of the digital memory unit are synchronized with the spectrometer magnetic field scan. To obtain a definite error signal indicating a mismatch, the wave form corresponding to ions of mass M_2 is subtracted. A synchronous dc-to-dc inverter stage with a gain that can be switched rapidly from $+1$ to -1 is used to obtain the positive wave form for mass M_1 and a negative wave form for mass M_2. Figure 2 shows the modified wave forms of Fig. 1 which are presented to the digital memory unit. The signal strengths of the two wave forms are attenuated separately to have the same intensity or area. If the two peaks have the same shape and the centers of area are superimposed, the stored signal will be zero plus the growth of random noise present on the mass peak signals. If the peaks are displaced, however, an error signal will grow linearly with the number of scans recorded in the memory while the average random noise will grow approximately as the square root of the number of scans. An exaggerated error signal is shown in Fig. 3(a) where the mismatch is again $+10\%$ as in Figs. 1 and 2. This signal corresponds to the average of 128 scans of each mass peak. Figure 3(b) shows an error signal corresponding to a mismatch of $+1\frac{1}{2}\%$, and Fig. 3(c) a mismatch corresponding to $-\frac{3}{4}\%$.


FIG. 2. A tracing of the mass peak wave forms of Fig. 1 here separately amplified and the wave form of $(Ba^{136})^+$ inverted. These signals are then presented to the digital memory oscilloscope.

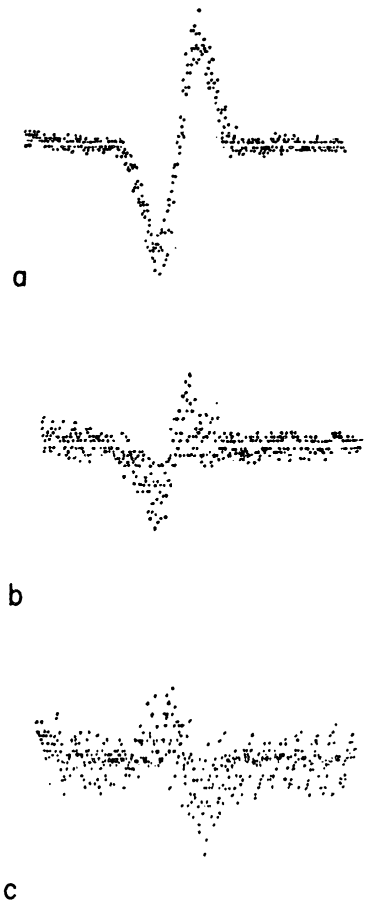

FIG. 3. A tracing of the error signal output of the digital memory oscilloscope corresponding to the accumulative algebraic signal from 128 sweeps of each mass wave form. In (a) the wave forms are mismatched by $+10\%$ of the width at half-maximum, in (b) the mismatch is $+1\frac{1}{2}\%$ and in (c) the mismatch is $-\frac{3}{4}\%$.

An individual peak-match setting for measurements described in this work has been made with a standard error of between 0.15 and 0.25% of the half-width W. One match using this new technique is equivalent to roughly 100 individual matches under the old visual technique on this spectrometer. The final probable error of the average after about 50 individual matchings now reduces to approximately 0.03% of the half-width W. The use of the memory averaging of peak-shape

---

[10] See, for example, M. P. Klein and G. W. Barton, Jr., Rev. Sci. Instr. **34**, 754 (1963).

[11] The digital memory oscilloscope employed is a model 800 Enhancetron, Nuclear Data Inc., Palatine, Illinois.

differences is approximately an order-of-magnitude improvement over our previous visual-matching method. In addition, it enables one to make accurate comparisons of peak shapes since a slight peak-shape difference, which would be visually undetectable because of the noise present on one scan of a peak, would become apparent when averaged over many scans.

The voltage divider used in previous work on this spectrometer was sufficiently precise so as to calculate voltage ratios on narrow doublet work. For wide mass doublets such as the single and double isotopic mass differences in the region of $A=150$, the previous voltage divider contributed the major error to the measurement. To measure such isotopic differences with a precision of 1 ppm requires a voltage divider capable of producing voltage ratios known to 1 ppm. A voltage divider of this precision was constructed. Tests and calibrations over a period of two years have shown it to be reliable to this precision.[12]

TABLE I. Mass doublets.

Doublet[a]	Measured mass difference[b] (u)	Error[c]	Adjusted mass difference[d] (u)	Error
$C_{11}H_{22}-C_{12}H_{10}$	0.093 902 7	4		
$C_3H_7Cl^{35}-C_3H_5Cl^{37}$	0.018 600 0	4	0.180 600 8	6
$C_6H_6-C_3H_7Cl^{35}$	0.023 320 8	3	0.023 321 2	6
$C_6H_6-C_3H_5Cl^{37}$	0.041 922 2	2	0.041 921 9	6
$Ba^{138}-Ba^{137}$	0.999 418	2	0.999 420	3
$Ba^{138}-Ba^{136}$	2.000 676	3	2.000 673	5
$Ba^{137}-Ba^{136}$	1.001 249	3	1.001 253	4
$Ba^{137}-Ba^{135}$	2.000 143	3	2.000 140	5
$Ba^{136}-Ba^{135}$	0.998 885	3	0.998 888	3
$Ba^{136}-Ba^{134}$	2.000 067	5	2.000 065	4
$Ba^{135}-Ba^{134}$	1.001 177	2	1.001 177	3
$Ba^{134}-Ba^{132}$	1.999 447	4	1.999 447	6
$Ba^{132}-Ba^{130}$	1.998 759	4	1.998 759	6
$C_{10}H_{18}-Ba^{138}$	0.235 609		0.235 603	12
$Ba^{135}-C_{10}H_{14}$	0.796 140		0.796 137	12
$C_{10}H_{14}-Ba^{134}$	0.205 025		0.205 041	12
$Ba^{134}-C_{10}H_{13}$	0.802 771		0.802 784	12
$Ce^{142}-Ce^{140}$	2.003 818	3		
$Ce^{140}-Ce^{138}$	1.999 457	8		
$Ce^{138}-Ce^{136}$	1.998 842	20		
$C_{11}H_{10}-Ce^{142}$	0.168 955		0.168 955	23
$C_{11}H_{10}-Ce^{140}$	2.172 765		2.172 775	23
$Ce^{142}-C_{11}H_9$	0.838 824		0.838 869	23
$C_{11}H_9-Ce^{140}$	1.164 956		1.164 949	23
$Nd^{150}-Nd^{148}$	2.003 988	3	2.003 988	7
$Nd^{148}-Nd^{146}$	2.003 773	3	2.003 773	5
$Nd^{146}-Nd^{145}$	1.000 536	2	1.000 539	4
$Nd^{146}-Nd^{144}$	2.003 026	3	2.003 020	5
$Nd^{145}-Nd^{144}$	1.002 480	2	1.002 481	4
$Nd^{145}-Nd^{143}$	2.002 751	3	2.002 755	5
$Nd^{144}-Nd^{143}$	1.000 273	2	1.000 274	4
$Nd^{144}-Nd^{142}$	2.002 366	3	2.002 361	5
$Nd^{143}-Nd^{142}$	1.002 084	2	1.002 087	4
$Nd^{143}-C_{11}H_{10}$	0.831 578		0.831 581	16
$Nd^{143}-C_{11}H_9$	1.839 406		1.839 406	16
$C_{11}H_{10}-Nd^{142}$	0.170 490		0.170 506	16
$Nd^{142}-C_{11}H_9$	0.837 335		0.837 319	16

[a] Throughout this work C and H refer to C^{12} and H^1.

[b] All masses measured in a scale where the mass of C^{12} is defined as exactly 12 units (symbol u).

[c] Throughout this work the errors refer to the last figure of the particular result.

[d] Where doublet data overdetermines the mass differences, the data is adjusted by a statistical least-squares process and the experimental errors are multiplied by the ratio of external to internal error to obtain the adjusted error. Unresolved systematic errors were observed in the metal-hydrocarbon doublets and these values were also adjusted to a consistent fit by least-squares analysis. The errors of these adjusted doublets are assigned to cover the magnitudes of the inconsistencies observed.

This new voltage divider along with the increased precision of the new peak-matching technique has made possible more accurate checks on spectrometer operation in the form of hydrocarbon mass unit measurements. A measurement of a mass difference of a doublet such as $C_mH_n-C_mH_{n-1}=\Delta m$ and $C_mH_n-C_mH_{n-2}=2\Delta m$ should give the hydrogen mass, Δm, if the spectrometer is properly focused and calibrated. During the course of the presently reported measurements, 16 such runs were made, giving a result of $\Delta m=1.007\,824\,7\pm10$.[13] The close agreement of this result with the more precise value of hydrogen reported in this paper ($1.007\,825\,22\pm3$ u) gives confidence in the reliability of other wide-doublet measurements.

MEASUREMENTS

Hydrogen

The major isotope of hydrogen is at present the most important secondary-mass standard. The use of C^{12} as a standard now permits the direct measurement of H^1 in a single doublet. The doublet measured for the determination of the hydrogen mass was $C_{11}H_{22}-C_{12}H_{10}=\Delta M_H$ which reduces to $H=\frac{1}{12}(C+\Delta M_H)$. The members of this doublet are molecular ions of the hydrocarbon compounds undecene and biphenyl, respectively. Choice of molecular ions eliminates a possible systematic error resulting from initial ion energy. The result of the doublet measurement is shown in Table I. This result is the average of five runs taken on five different days spanning a period of two months. Statistical analysis of each run indicated a standard deviation from peak-matching of ±0.6 μu. The total spread of the five runs was 1.5 μu and the error associated with the peak-matching statistics of the five runs was ±0.3 μu. The final error is obtained by combining this statistical error with the error from the resistor calibration. Considered in this measurement is the possible effect of differing molecular binding energy in the two molecules making up the doublet. This energy difference is estimated to be about 27 eV, less than $\frac{1}{10}$ of the quoted doublet error, and has thus been neglected.

The value of the hydrogen mass calculated from this doublet is shown in Table II. Also shown is the value (b) calculated from previous measurements[4] on the same spectrometer at this laboratory as well as a value (c) calculated from measurements obtained by Smith[14] employing a mass synchrometer. The disagreement

---

[12] *Nuclidic Masses*, edited by Walter H. Johnson, Jr. (Springer-Verlag, Vienna, 1964), p. 375.

[13] Errors refer to the last figure of the quoted result.

[14] Lincoln G. Smith, Phys. Rev. **111**, 1606 (1958).

TABLE II. Atomic masses.

	Present result		1964 mass table[a]		Other values	
Isotope	(u)	Error (μu)	(u)	Error (μu)	(u)	Error (μu)
H^1	1.007 825 22	0.03	1.007 825 19	0.08	1.007 824 70	0.20[b]
					1.007 824 93	0.30[c]
Cl^{35}	34.968 853 6	0.6	34.968 851 1	1.3	34.968 856 2	1.4[d]
					34.968 872 8	4.7[c]
					34.968 851 38	0.68[e]
Cl^{37}	36.965 903 3	0.6	36.965 898 5	1.1	36.965 904 0	1.2[d]
					36.965 886 6	3.6[c]
					36.965 900 27	0.95[e]
$Cl^{37}-Cl^{35}$	1.997 049 7	0.6	1.997 047 4	1.7	1.997 047 8	1.8[d]
					1.997 013 8	5.9[c]
					1.997 048 89	0.59[e]
Ba^{130}	129.906 307	11	129.906 245	23	129.906 809	210[f]
Ba^{132}	131.905 066	10	131.905 120	300	131.905 128	120[f]
Ba^{134}	133.904 513	8	133.904 612	41	133.904 261	80[f]
Ba^{135}	134.905 690	8	134.905 550	110	134.905 571	98[f]
Ba^{136}	135.904 578	8	135.904 300	80	135.904 380	86[f]
Ba^{137}	136.905 831	8	136.905 500	80	136.905 545	57[f]
Ba^{138}	137.905 251	8	137.905 000	60	137.904 899	77[f]
Ce^{136}	135.907 179	24	135.907 100	500	135.907 082	200[f]
Ce^{138}	137.906 021	14	137.905 830	60	137.906 035	200[f]
Ce^{140}	139.905 478	12	139.905 392	19	139.905 290	60[f]
Ce^{142}	141.909 296	12	141.909 140	50	141.909 309	68[f]
Nd^{142}	141.907 746	8	141.907 663	16	141.907 496	30[f]
Nd^{143}	142.909 833	8	142.909 779	15	142.909 585	100[f]
Nd^{144}	143.910 107	9	143.910 039	15	143.909 804	67[f]
Nd^{145}	144.912 588	9	144.912 538	15	144.912 062	190[f]
Nd^{146}	145.913 127	9	145.913 086	15	145.912 691	57[f]
Nd^{148}	147.916 900	10	147.916 869	15	147.916 473	58[f]
Nd^{150}	149.920 888	13	149.920 915	15	149.920 826	71[f]

[a] Reference 16.
[b] Reference 4.
[c] Value calculated from values given in Ref. 14 converted to C^{12} scale and errors multiplied by ratio of external to internal error as suggested by author.
[d] Reference 5.
[e] Reference 18.
[f] Masses calculated from values given in Ref. 19 converted to C^{12} scale.

between the present value and the previous Minnesota value appears to be consistent with the finding of König *et al.*[15] that the ratio of external to internal error was 2.65 (i.e., the quoted errors are too small by a factor of 2.65) for the doublets measured at the time the previous result was obtained. The value from the 1964 mass table of Mattauch *et al.*,[16] is from a consistent list of nuclidic masses computed by least-squares methods from all significant experimental mass measurements and reaction data available up to 1963. The agreement between this value and the present result is seen to be very good.

Chlorine

The mass of Cl^{35}, Cl^{37}, and the $Cl^{37}-Cl^{35}$ mass difference have taken on greater importance since the introduction of a new set of mass doublets by Duckworth and co-workers.[17] These doublets measure the mass difference between two isotopes of an element differing by two mass numbers, X^A and X^{A+2}. The doublet measured is $X^ACl^{37}-X^{A+2}Cl^{35}$. In order to derive the mass difference $X^{A+2}-X^A$, an accurate $Cl^{37}-Cl^{35}$ mass difference must be available. The uncertainty in the $Cl^{37}-Cl^{35}$ mass difference has in fact contributed a large share of the total error attached to the calculation of the mass difference $X^{A+2}-X^A$ from the very precise doublets measured by Duckworth and co-workers.

The $Cl^{37}-Cl^{35}$ mass value had been derived by Mattauch *et al.*,[16] from a least-squares fit of the available mass spectroscopic and nuclear reaction data. Some of the input data which go into the least-squares fit are the mass spectroscopic doublets measured by Giese and Benson[5] and the mass synchrometer doublet measured by Smith.[14] A large disagreement between these two sets of doublet measurements resulted in the rejection by Mattauch *et al.* of both sets in the 1964 mass table. Smith notes that the value of one of his doublets, C_3H-Cl^{37}, is probably in error due to initial kinetic energy in one of the members of the doublet. In order to further study this disagreement, a new set of chlorine doublets was measured.

The chlorine masses were obtained from the three mass doublet measurements of the triad at mass 78; benzene (C_6H_6), isopropyl chloride ($C_3H_7Cl^{35}$), and propenyl chloride ($C_3H_5Cl^{37}$). Again the doublet members are all simple molecular ions. The measured mass differences are shown in Table I. Since the doublet mass differences are overdetermined by this set of measure-

---

[15] L. A. König, J. H. E. Mattauch, and A. H. Wapstra, Nucl. Phys. **31**, 18 (1962).

[16] J. H. E. Mattauch, W. Thiele, and A. H. Wapstra, Nucl. Phys. **67**, 1 (1965).

[17] R. C. Barber, H. E. Duckworth, B. G. Hogg, J. D. Macdougall, W. McLatchie, and P. Van Rookhuyzen, Phys. Rev. Letters **12**, 597 (1964).

ments, a least-squares adjustment of the measured values was performed. The resulting adjusted values are also shown in Table I. The errors associated with the adjusted values were obtained by multiplying the final statistical errors by 2.5, the ratio of the external to internal errors calculated from the least-squares adjustment. The calculated mass values shown in Table II are seen to be in reasonable agreement with previous Minnesota values (d). The disagreement with the values of Smith (c) may in part be explained by the initial energies previously mentioned. The value of Mattauch *et al.*, is obtained from a least-squares analysis of mass measurement and reaction data. Also listed are the new values measured by Dewdney and Bainbridge.[18] The agreement between the present results and those of Dewdney and Bainbridge are in each case reasonably good. In particular, the agreement between the two values of the $Cl^{37}-Cl^{35}$ mass difference is very good.

Barium

Sufficient intensity to run even the two rare isotopes was obtained from barium vapor. Single and double isotopic mass differences were measured and the values obtained are shown in Table I. Since the set of measurements overdetermines the set of isotopic differences sought, a least-squares analysis of the data was performed. The adjusted values of these data are also shown in Table I. The ratio of external-to-internal error in this analysis was 1.8 and the quoted errors in the adjusted values have been multiplied by this factor. To minimize the chance of systematic error due to possible dissimilarity in the spatial distributions of the barium and hydrocarbon ion currents, four different doublet measurements were made and combined with the previously calculated isotopic differences to obtain four adjusted and consistent values. Errors were assigned equally to each barium-hydrocarbon result.

Neodymium

Neodymium ions were obtained from the vapor of $NdCl_3$. The isotopic doublet measurements are shown in Table I. Also shown are the adjusted-mass-difference values which are obtained from a least-squares analysis. The errors quoted in the adjusted values are obtained by multiplying the calculated final errors by 2.5, the ratio of external-to-internal error for this set of data.

The neodymium-hydrocarbon doublets are also shown in Table I. Again, an overdetermined set of doublets was measured to minimize systematic errors. In these measurements it was noted that the Nd^{142} peak was very slightly wider than either of the hydrocarbon comparison peaks. The detection of this 2% peak shape difference was made possible by the very precise method of signal averaging in the digital memory device. This difference was at first thought to be caused by ion source discrimination between the two types of molecules. However, the least-squares adjustment of this data combined with the isotopic mass difference and the known mass of the comparison hydrocarbon ions indicates a systematic error in both of the Nd^{142} runs of about 16 μu. A calculation indicates that if a Ce^{142} contaminant of approximately 1% of the Nd^{142} intensity were present, the observed peak widening and the 16 μu error indicated in the two Nd^{142}-hydrocarbon runs would be explained. To cover the possibility that this explanation is not correct, a 16-μu error was assigned to each of the four neodymium-hydrocarbon runs. While the source of this contaminant is not known, it is our belief that this contaminant, if it existed, was not present in the previously discussed isotopic doublet measurements, since no peak-shape differences were observed.

Cerium

The cerium ions were obtained from the vapor of $CeCl_3$. The doublet mass differences measured are listed in Table I. Sufficient intensity for the Ce^{140} and Ce^{142} doublets was easily obtained. However, it was extremely difficult to obtain sufficient intensity for the two rare isotopes of Ce^{136} and Ce^{138}. It was necessary to run the $Ce^{140}-Ce^{138}$ doublet by the visual peak-matching method because of the large intensity difference in these two ion beams. Difficulties due to poor intensity of both members of the $Ce^{138}-Ce^{136}$ doublet is reflected in the large error assigned to this measurement.

The four cerium-hydrocarbon doublets result in an over determined set of data which was analyzed by least-squares fitting. The rather large adjustment needed in the $Ce^{142}-C_{11}H_9$ doublet value would be consistent with an error produced by a Nd^{142} contaminant under the Ce^{142} peak. However, checks were made before these runs to prove the absence of such a contaminant and this large error may be further evidence of systematic errors due to dissimilarity in the spatial distribution of ion currents from such different vapor sources.

Atomic Masses

Listed in Table II are the atomic masses calculated from the doublet results given in Table I. All masses are calculated using the mass scale in which C^{12} equals exactly 12 u. Also listed in Table II (f) are the barium, cerium, and neodymium isotopic masses calculated from previous Minnesota measurements[19] made on a smaller spectrometer and masses included in the 1964 mass table of Mattauch *et al.*[16] The previous Minnesota values are in reasonable agreement with the present values for the barium and cerium isotopes but seem to be consistently lower in the case of the neodymium masses. There also seems to be generally poor agreement between the 1964 mass table values and the

---

[18] J. W. Dewdney and K. T. Bainbridge, Phys. Rev. **138**, B540 (1965).

[19] W. H. Johnson, Jr., and A. O. Nier, Phys. Rev. **105**, 1014 (1957).

TABLE III. Chlorine narrow-doublet mass differences.

Doublet	Present results[a] (μu)	Barber *et al.*[b] (μu)	Difference (μu)
$Nd^{144}Cl^{35}-Nd^{142}Cl^{37}$	5311±5	5329±3	18±6
$Nd^{145}Cl^{35}-Nd^{143}Cl^{37}$	5705±5	5744±5	39±7
$Nd^{146}Cl^{35}-Nd^{144}Cl^{37}$	5970±5	6003±3	33±6
$Nd^{148}Cl^{35}-Nd^{146}Cl^{37}$	6723±5	6740±4	17±6
$Nd^{150}Cl^{35}-Nd^{148}Cl^{37}$	6938±7	7006±5	68±9

[a] Calculated from isotopic doublet values in Table I along with the present value of $Cl^{37}-Cl^{35}$ given in Table II.
[b] Reference 17.

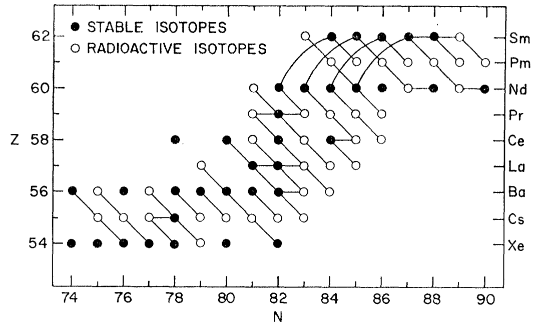

FIG. 4. Nuclear reaction, alpha-decay and beta-decay paths that were employed to calculate additional atomic masses. Solid circles represent stable isotopes, and open circles represent radioactive isotopes. Connecting lines indicate reaction or decay path.

present values. For barium and cerium the differences seem to be random and probably reflect the lack of accuracy of the input measurements used in compiling the mass table. The mass table values for neodymium have 15-μu errors and average about 50 μu higher than the present values. These small quoted errors probably result in part from the precise values of some NdCl isotopic doublets measured by Barber *et al.*,[17] as shown in Table III. It is seen that the values of Barber *et al.*, are all significantly higher than the presently reported values. In view of the internal consistency of the presently reported neodymium isotopic and hydrocarbon doublets, no errors in this present work seem to be of magnitude great enough to explain this discrepancy.

Nuclear Systematics

The nuclear-reaction, alpha-decay, and beta-decay paths used in the calculation of the additional atomic masses are shown in Fig. 4. The conversion[20] 931.478 ±0.004 MeV/u has been used to convert Q value and disintegration energies to C^{12} mass units. The value of $H=1.007\,825\,22\pm3$ from this work and the values

$$n=1.008\,665\,2\pm1\,,$$
$$D=2.014\,102\,2\pm1\,,$$
$$He^4=4.002\,603\,1\pm4$$

from Ref. 16 have been used in calculating the mass differences. The atomic masses calculated from the reaction paths are given in Table IV.

Some of the resulting mass links are overdetermined but inconsistent. In other cases, the resulting mass links are uniquely determined but apparently wrong. For the two paths leading to the Cs^{136} mass, the $Cs^{136}(\beta^-)Ba^{136}$ Q value was rejected since the nuclear systematics resulting from this path were clearly wrong. A similar choice was made in the case of the two paths leading to the Nd^{147} mass. Here, the $Nd^{148}(\gamma,n)-Nd^{147}$ path also gave nuclear systematic energies deviating from those to be expected and was rejected. In the closed cycle of paths involving Ce^{141}, the $Ce^{140}(d,p)Ce^{141}$ reaction was rejected as being inconsistent with the other reaction paths and also giving atypical nuclear systematics. The two alpha-decay energies of Sm^{147} could be considered as consistent and a weighted average taken; however, the one value which was finally used gives much more reasonable systematic energies. The $Pm^{146}(\beta^-)Sm^{146}$ Q value quoted in the nuclear data sheet reference gave a mass for Pm^{146} which was obviously wrong from a study of the resulting nuclear systematics. If one assumes that the Pm^{146} decays to the first 2^+ level of Sm^{146} rather than the 0^+ ground state, the resulting disintegration energy gives a Pm^{146} mass which agrees very well with expected nuclear systematics in this region. This new disintegration energy is the one quoted in Table IV and used for the mass calculation. Some other reaction paths are also considered to be unreliable, but have been employed since no other means of calculation is available. These cases will be pointed out in the following discussions of nuclear systematics.

In studies of nuclear systematics, it is more profitable to consider differences in nuclear binding energy between neighboring nuclei rather than to consider the systematics of the total nuclear binding. Differences such as the neutron separation energy $S_n(Z,N)$, the separation energy of the last two neutrons $S_{2n}(Z,N)$ and the neutron pairing energy $P_n(Z,N)$, given by the following expressions, prove to be useful.

$$S_n(Z,N)=M(Z,\,N-1)+M(0,1)-M(Z,N),$$
$$S_{2n}(Z,N)=M(Z,\,N-2)+2M(0,1)-M(Z,N),\quad (N\text{ even})$$
$$P_n(Z,N)=S_n(Z.N)-S_n(Z,\,N-1),\quad (N\text{ even}).$$

Similar relationships hold for the proton systematics except in this case differences in atomic-binding energy from element to element need to be considered. We have employed the approximate relationship[21] that the total electronic binding energy is equal to $1.689\times10^{-8}\mathrm{u}\times Z^{7/3}$. Listed in Tables V and VI are the neutron and proton separation and pairing energies which were calculated from the atomic masses given in Tables II and IV.

---

[20] *Nuclidic Masses*, edited by Walter H. Johnson, Jr. (Springer-Verlag, Vienna, 1964), p. 101.

[21] L. L. Foldy, Phys. Rev. 83, 397 (1951).

These quantities are plotted in Figs. 5–10 and are discussed below.

Before discussing the individual graphs, it will be best to point out some of the features common to many of them which lead to the suspicion of errors in some of the reaction Q values used in the mass calculations. The

TABLE IV. Atomic masses calculated from nuclear-reaction mass links and from masses in Table V and Xe masses.[a]

Isotope	Reaction	Q value[b] (μu)	Error (μu)	Reference[c]	Mass (u)	Error (μu)
Xe^{133}	$\mathrm{Xe}^{133}(\beta^-)\mathrm{Cs}^{133}$	459	4	61-2-88	132.905 875	56
Cs^{130}	$\mathrm{Cs}^{130}(\beta^+)\mathrm{Xe}^{130}$	3210	54	61-3-75	129.906 713	54
	$\mathrm{Cs}^{130}(\beta^-)\mathrm{Ba}^{130}$	453	1	61-3-75	129.906 760	12
					129.906 757	11[d]
Cs^{131}	$\mathrm{Cs}^{131}(\beta^+)\mathrm{Xe}^{131}$	381	6	61-2-60	130.905 461	7
Cs^{132}	$\mathrm{Cs}^{132}(\beta^+)\mathrm{Xe}^{132}$	2244	27	[e]	131.906 400	27
Cs^{133}	$\mathrm{Cs}^{133}(\gamma,n)\mathrm{Cs}^{132}$	−9649	35	61-2-90	132.905 416	44
Cs^{134}	$\mathrm{Cs}^{134}(\beta^-)\mathrm{Ba}^{134}$	2212	11	61-2-104		
	$\mathrm{Cs}^{134}(\beta^-)\mathrm{Be}^{134}$	2209	5	[f]		
		2210	5[d]		133.906 722	10
Cs^{135}	$\mathrm{Cs}^{135}(\beta^-)\mathrm{Ba}^{135}$	225	5	61-2-118	134.905 915	9
Cs^{136}	$\mathrm{Cs}^{136}(\beta^+)\mathrm{Xe}^{136}$	204	11	61-2-126	135.907 417	12
	$\mathrm{Cs}^{136}(\beta^-)\mathrm{Ba}^{136}$	3038	11	61-2-126	135.907 616	14
					135.907 417	12[g]
Cs^{137}	$\mathrm{Cs}^{137}(\beta^-)\mathrm{Ba}^{137}$	1263	2	61-2-133	136.907 094	8
Cs^{138}	$\mathrm{Cs}^{138}(\beta^-)\mathrm{Ba}^{138}$	5185	11	61-3-80	137.910 436	14
Ba^{131}	$\mathrm{Ba}^{131}(\beta^+)\mathrm{Cs}^{131}$	1250	5	[h]	130.906 711	9
Ba^{133}	$\mathrm{Ba}^{133}(\beta^+)\mathrm{Cs}^{133}$	524	5	61-2-91	132.905 940	44
Ba^{139}	$\mathrm{Ba}^{138}(d,p)\mathrm{Ba}^{139}$	2676	11	61-3-91		
	$\mathrm{Ba}^{139}(\beta^-)\mathrm{La}^{139}$	2512	43	61-3-90		
	$\mathrm{La}^{139}(\gamma,n)\mathrm{La}^{138}$	−9420	27	61-3-92		
	$\mathrm{La}^{138}(\beta^-)\mathrm{Ce}^{138}$	1090	16	61-3-82		
	$\mathrm{Ba}^{139}(\beta^-)\mathrm{La}^{139}$	2512	43	61-3-90		
	$\mathrm{La}^{139}(d,p)\mathrm{La}^{140}$	3070	32	[i]		
	$\mathrm{La}^{140}(\beta^-)\mathrm{Ce}^{140}$	4080	32	59-1-89	138.908 855	13[j]
Ba^{140}	$\mathrm{Ba}^{140}(\beta^-)\mathrm{La}^{140}$	1127	11	59-1-87	139.910 698	29
La^{136}	$\mathrm{La}^{136}(\beta^+)\mathrm{Ba}^{136}$	3081	75	61-2-127	135.907 659	75
La^{138}					137.907 129	18[j]
La^{139}					138.906 371	21[j]
La^{140}					139.909 571	27[j]
La^{141}	$\mathrm{La}^{141}(\beta^-)\mathrm{Ce}^{141}$	2609	32	61-4-32	140.910 926	48
La^{142}	$\mathrm{La}^{142}(\beta^-)\mathrm{Ce}^{142}$	4842	32	[k]	141.914 139	36
Ce^{139}	$\mathrm{Ce}^{139}(\beta^+)\mathrm{La}^{139}$	290	6	61-3-93	138.906 661	22
Ce^{141}	$\mathrm{Ce}^{140}(d,p)\mathrm{Ce}^{141}$	3446	32	61-4-34	140.908 317	36
	$\mathrm{Ce}^{141}(\beta^-)\mathrm{Pr}^{141}$	623	5	61-4-33	140.908 203	30
					140.908 203	30[l]
Ce^{143}	$\mathrm{Ce}^{142}(d,p)\mathrm{Ce}^{143}$	3070	75	61-4-45	142.912 504	77
	$\mathrm{Ce}^{143}(\beta^-)\mathrm{Pr}^{143}$	1546	11	61-4-44	142.912 381	15
					142.912 386	15[d]
Ce^{144}	$\mathrm{Ce}^{144}(\beta^-)\mathrm{Pr}^{144}$	344	11	59-1-111	143.913 650	18
Pr^{140}	$\mathrm{Pr}^{140}(\beta^+)\mathrm{Ce}^{140}$	3489	22	59-1-94		
	$\mathrm{Ce}^{140}(d,p)\mathrm{Ce}^{141}$	3446	32	61-4-34		
	$\mathrm{Ce}^{141}(\beta^-)\mathrm{Pr}^{141}$	623	5	61-4-33		
	$\mathrm{Pr}^{141}(\gamma,n)\mathrm{Pr}^{140}$	−10059	21	61-4-35		
	$\mathrm{Pr}^{141}(d,p)\mathrm{Pr}^{142}$	3800	43	[i]		
	$\mathrm{Pr}^{142}(\beta^-)\mathrm{Nd}^{142}$	2311	9	59-1-101	139.908 975	22[m]
Pr^{141}					140.907 581	28[m]
Pr^{142}					141.910 057	12[m]
Pr^{143}	$\mathrm{Pr}^{143}(\beta^-)\mathrm{Nd}^{143}$	1002	5	61-4-46	142.910 835	10
Pr^{144}	$\mathrm{Pr}^{144}(\beta^-)\mathrm{Nd}^{144}$	3199	11	59-1-113	143.913 306	14
Pr^{145}	$\mathrm{Pr}^{145}(\beta^-)\mathrm{Nd}^{145}$	1932	11	59-1-120	144.914 520	14
Nd^{141}	$\mathrm{Nd}^{141}(\beta^+)\mathrm{Pr}^{141}$	1932	11	61-4-36	140.909 513	30
Nd^{147}	$\mathrm{Nd}^{147}(\beta^-)\mathrm{Pm}^{147}$	966	5	59-1-136	146.916 102	23
	$\mathrm{Nd}^{148}(\gamma,n)\mathrm{Nd}^{147}$	6785	160	61-4-55	146.915 020	160
					146.916 102	23[n]
Nd^{149}	$\mathrm{Nd}^{150}(\gamma,n)\mathrm{Nd}^{149}$	−7912	86	5-6-9	148.920 136	87
	$\mathrm{Nd}^{149}(\beta^-)\mathrm{Pm}^{149}$	1718	54	5-2-19	148.920 034	76
					148.920 077	57[d]

[a] Xe masses taken from Ref. 7.

[b] 931.476±0.004 MeV/u from Ref. 20 used to convert Q value energies.

[c] References to the *Nuclear Data Sheets* are given as year, set, and page number. For recent editions the volume number rather than the year is given.

[d] Weighted average.

[e] R. L. Robinson, Noah R. Johnson, and E. Eichler, Phys. Rev. **128**, 252 (1962).

[f] W. Van Wijngaarden and R. D. Conner, Can. J. Phys. **42**, 504 (1964).

[g] The $\mathrm{Cs}^{136}(\beta^-)\mathrm{Ba}^{136}$ Q value is rejected as giving inconsistent nuclear systematic energies.

[h] R. L. Robinson, Bull. Am. Phys. Soc. **7**, 562 (1962).

[i] F. W. Bingham and M. B. Sampson, Phys. Rev. **128**, 1796 (1962).

[j] Weighted average from analysis of various dependent and independent paths resulting from the indicated reactions listed under Ba^{139}.

[k] W. V. Prestwich and T. J. Kennett, Phys. Rev. **134B**, 485 (1964).

[l] The $\mathrm{Ce}^{140}(d,p)\mathrm{Ce}^{141}$ reaction path is rejected as giving inconsistent mass and nuclear systematic energies.

[m] Weighted average from analysis of various dependent and independent paths resulting from the indicated reactions listed under Pr^{140}.

[n] The $\mathrm{Nd}^{148}(\gamma,n)\mathrm{Nd}^{147}$ Q value was rejected as giving nuclear systematic energies which clearly deviate from those to be expected.

Table IV (*continued*)

Isotope	Reaction	Q value[b] (μu)	Error (μu)	Reference[c]	Mass (u)	Error (μu)
Pm^{145}	$\mathrm{Pm}^{145}(\beta^+)\mathrm{Nd}^{145}$	150	11	59-1-122	144.912 738	14
Pm^{146}	$\mathrm{Pm}^{146}(\beta^-)\mathrm{Sm}^{146}$	1605[o]	107	59-1-129	145.914 799	120
Pm^{147}	$\mathrm{Pm}^{147}(\beta^-)\mathrm{Sm}^{147}$	242	1	59-1-138	147.915 136	22
Pm^{148}	$\mathrm{Pm}^{148}(\beta^-)\mathrm{Sm}^{148}$	2630	21	61-4-56	147.917 702	39
Pm^{149}	$\mathrm{Pm}^{149}(\beta^-)\mathrm{Sm}^{149}$	1150	2	5-2-20	148.918 379	55
	$\mathrm{Nd}^{149}(\beta^-)\mathrm{Pm}^{149}$	1718	54	5-2-19	148.918 417	102
					148.918 387	48[d]
Pm^{150}	$\mathrm{Pm}^{150}(\beta^-)\mathrm{Sm}^{150}$	3682	64	5-6-10	149.921 003	81
Pm^{151}	$\mathrm{Pm}^{151}(\beta^-)\mathrm{Sm}^{151}$	1283	11	5-5-6	150.921 326	82
Sm^{145}	$\mathrm{Sm}^{145}(\beta^+)\mathrm{Pm}^{145}$	687	21	59-1-123	144.913 425	25
Sm^{146}	$\mathrm{Sm}^{146}(\alpha)\mathrm{Nd}^{142}$	2845	54	59-1-130	145.913 194	54
	$\mathrm{Pm}^{146}(\beta^-)\mathrm{Sm}^{146}$	805	107	59-1-129	145.913 331	173
					145.913 208	51[d]
Sm^{147}	$\mathrm{Sm}^{147}(\alpha)\mathrm{Nd}^{143}$	2339	32	59-1-139	146.914 775	33
	$\mathrm{Sm}^{147}(\alpha)\mathrm{Nd}^{143}$	2548	21	[p]	146.914 894	22
					146.914 894	22[q]
Sm^{148}	$\mathrm{Sm}^{148}(\alpha)\mathrm{Nd}^{144}$	2362	32	61-4-60	147.915 072	33
Sm^{149}	$\mathrm{Sm}^{149}(\alpha)\mathrm{Nd}^{145}$	2029	54	5-2-21	148.917 220	54
	$\mathrm{Pm}^{149}(\beta^-)\mathrm{Sm}^{149}$	1150	2	5-2-20	148.917 267	103
					148.917 229	49[d]
Sm^{150}	$\mathrm{Sm}^{149}(n,\gamma)\mathrm{Sm}^{150}$	8570	4	5-6-13	149.917 324	49
	$\mathrm{Sm}^{149}(d,p)\mathrm{Sm}^{150}$	6188	4	5-2-21	149.917 318	49
					149.917 321	49[d]
Sm^{151}	$\mathrm{Sm}^{150}(d,p)\mathrm{Sm}^{151}$	3552	17	5-5-14	150.920 043	52

[o] Assuming Pm^{146} decays to the first excited 2^+ level rather than the 0^+ ground state as given in the reference.
[p] R. D. Macfarlane and T. P. Kohman, Phys. Rev. **121**, 1758 (1961).
[q] The lower energy decay energy was rejected as giving atypical nuclear systematic energies.

values of $S_n(55,83)$ and $S_p(56,83)$ are, respectively, too high and too low. These could both be explained by a 500-μu error in the $\mathrm{Cs}^{138}(\beta^-)\mathrm{Ba}^{138}$ disintegration energy shown in Table IV. This energy was calculated from an assumed level scheme for Ba^{138} which by the above reasoning now appears to be in error. The high values of $S_n(57,85)$, $S_n(59,85)$, $S_n(58,86)$, and $S_p(60,84)$ and the low value of $P_n(59,86)$ might all be explained by an error in the $\mathrm{Pr}^{143}(\beta^-)\mathrm{Nd}^{143}$ disintegration energy.

Neutron separation energies are plotted as a function of N in Fig. 5. The most striking feature of this graph is the sharp decrease in neutron separation energy after the shell closure at 82 neutrons. While the average slope before and after this closure is approximately -180 μu/neutron, the slope at the closure is approximately -1080 μu per neutron. Thus the energy gap at this closure is approximately 900 μu. The separation energies increase for increasing Z with the exception of the previously discussed points for cesium at $N=83$, lanthanum and praesodymium at $N=85$, cerium at $N=86$ (where these points are thought to be too high because of Q-value errors), and the point at $N=89$ for promethium. For further evaluation of this increase see the discussion of proton separation energies. The higher than expected separation energies in the region of 88, 89, and 90 neutrons may be evidence for slightly greater binding due to collective motions of some of these last added nucleons. This effect was first observed by Hogg and Duckworth,[22] later by Johnson and Nier,[19] and more recently by Barber *et al.*,[17] Barber *et al.*, found this increased binding to start an $N=89$ and to be more pronounced the higher the value of Z. The present graph seems to follow this in comparing values for neodymium to those of promethium but the effect is not at all indicated for the samarium values. This may be due to incorrect Q values used to calculate the systematics involving the samarium isotopes since Barber *et al.*, found a pronounced effect at $N=89$ for samarium.

The separation energy of the last two neutrons is plotted as a function of N in Fig. 6. The regularity of the curves preceding the shell closure at 82 neutrons and the sharp discontinuity at the shell closure are especially pronounced in this graph. Also to be noted is the break in the curves at 88 neutrons again indicating a rather large change in neutron binding which occurs at either 89 or 90 neutrons in neodymium and promethium.

The neutron pairing energies are shown as a function

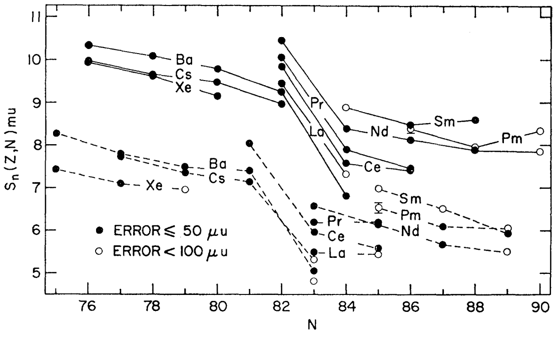

Fig. 5. Neutron separation energies as a function of N.

---

[22] B. G. Hogg and H. E. Duckworth, Phys. Rev. **91**, 1289 (1953).

TABLE V. Neutron separation and pairing energies.

		S_n		S_{2n}		P_n	
Element	N	(mu)	Error (μu)	(mu)	Error (μu)	(mu)	Error (μu)
Xe	75	7.415	6				
	76	9.941	7	17.356	6	2.256	9
	77	7.088	7				
	78	9.589	6	16.677	6	2.501	9
	79	6.946	56				
	80	9.150	56	16.096	6	2.204	112
	82			15.507	6		
Cs	76	9.961	13				
	77	7.726	28				
	78	9.649	35	17.375	44	1.923	45
	79	7.359	45				
	80	9.472	13	16.831	41	2.113	47
	81	7.164	15				
	82	8.988	14	16.151	7	1.824	27
	83	5.323	55				
Ba	75	8.261	13				
	76	10.310	13	18.571	6	2.049	18
	77	7.791	45				
	78	10.093	45	17.884	6	2.302	64
	79	7.487	3				
	80	9.777	3	17.264	5	2.290	4
	81	7.412	4				
	82	9.245	3	16.657	5	1.833	5
	83	5.061	14				
	84	6.822	35	11.883	33	1.762	38
La	82	9.423	21				
	83	5.465	32				
	84	7.309	57	12.775	52	1.845	65
	85	5.452	60				
Ce	80			18.488	20		
	81	8.032	29				
	82	9.840	28	17.872	8	1.808	39
	83	5.948	34				
	84	7.571	20	13.509	3	1.623	45
	85	5.576	22				
	86	7.401	23	12.977	25	1.825	29
Pr	82	10.060	21				
	83	6.188	32				
	84	7.887	15	14.075	31	1.699	34
	85	6.194	17				
	86	7.451	20	13.645	17	1.257	20
Nd	82	10.432	31				
	83	6.578	4				
	84	8.391	4	14.969	5	1.813	6
	85	6.184	4				
	86	8.126	4	14.310	5	1.942	6
	87	5.690	24				
	88	7.867	24	13.557	5	2.177	45
	89	5.488	58				
	90	7.854	58	13.342	7	2.366	82
Pm	85	6.524	120				
	86	8.408	120	14.932	36	1.884	170
	87	6.099	45				
	88	7.980	62	14.079	58	1.881	80
	89	6.049	94				
	90	8.342	114	14.391	95	2.293	147
Sm	84	8.882	57				
	85	6.979	56				
	86	8.487	40	15.466	61	1.508	71
	87	6.508	59				
	88	8.573	2	15.081	59	2.065	59
	89	5.943	17				

of N in Fig. 7. Mayer and Jensen[23] indicate that the value of the pairing energy should increase with the value of spin of the level which the two nucleons enter. However, this level need not be the one occupied by the previous odd nucleon. According to Mayer and Jensen[23] the expected configuration of energy levels just below the shell closure at $N=82$ is $1h^{11/2}(12)$, $2d^{3/2}(4)$. Thus the pairing at $N=82$ and $N=80$ must occur in the $j=\frac{3}{2}$ level since the lower $j=11/2$ level will be filled first. From the graph it is seen that the pairing energies are quite similar for the three elements at each of these points but are about 400 μu higher at $N=80$ than at $N=82$. This may indicate that at $N=80$ there is

TABLE VI. Proton separation and pairing energies.

		S_p		S_{2p}		P_p	
N	Z	(mu)	Error (μu)	(mu)	Error (μu)	(mu)	Error (μu)
74	56			12.853	12		
75	55	5.837	12				
	56	7.861	14	13.699	9	2.024	18
76	55	5.857	9				
	56	8.210	12	14.068	11	2.353	15
77	55	6.495	28				
	56	8.275	52	14.771	44	1.780	59
78	55	6.555	44				
	56	8.719	45	15.275	9	2.164	63
	58			12.956	29		
79	55	6.968	57				
	56	8.847	12	15.816	56	1.879	58
	57	5.846	75				
80	55	7.290	10				
	56	9.152	12	16.443	9	1.862	16
	58			14.180	21		
81	56	9.401	14				
	57	6.517	19				
	58	8.283	22	14.800	23	1.766	29
	59	5.500	31				
	60	7.276	44	12.777	37	1.776	54
82	55	7.934	9				
	56	9.658	11	17.593	9	1.724	14
	57	6.695	22				
	58	8.700	27	15.395	19	2.005	35
	59	5.719	33				
	60	7.649	28	13.369	19	1.930	44
83	56	9.396	55				
	57	7.099	33				
	58	9.183	40	16.282	32	2.084	52
	59	5.960	32				
	60	8.038	9	13.999	31	2.078	33
	62			12.036	26		
84	57	7.587	58				
	58	9.444	51	17.031	34	1.857	77
	59	6.276	20				
	60	8.542	6	14.819	19	2.266	21
	61	5.183	17				
	62	7.343	53	12.527	52	2.160	56
85	58	9.568	39				
	59	6.894	21				
	60	8.532	12	15.427	17	1.638	24
	61	5.523	120				
	62	7.798	120	13.322	25	2.275	170
86	59	6.944	23				
	60	9.207	12	16.152	24	2.263	26
	61	5.805	23				
	62	7.877	42	13.683	34	2.072	49
87	61	6.214	45				
	62	8.286	62	14.401	54	2.072	78
88	61	6.327	49				
	62	8.879	68	15.207	50	2.552	84
89	61	6.888	99				
	62	8.773	96	15.662	75	1.885	135
90	61	7.376	83				

---

[23] M. G. Mayer and J. H. D. Jensen, *Elementary Theory of Nuclear Shell Structure* (John Wiley & Sons, Inc., New York, 1955).

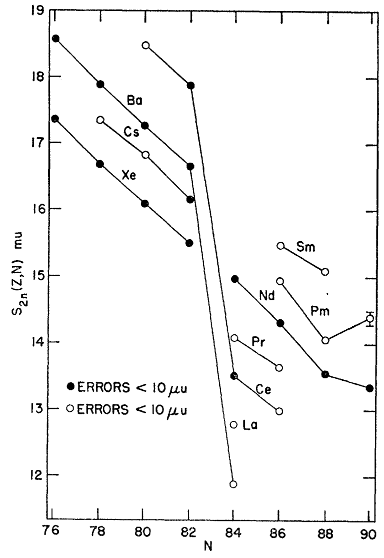

FIG. 6. Separation energy of the last two neutrons as a function of N.

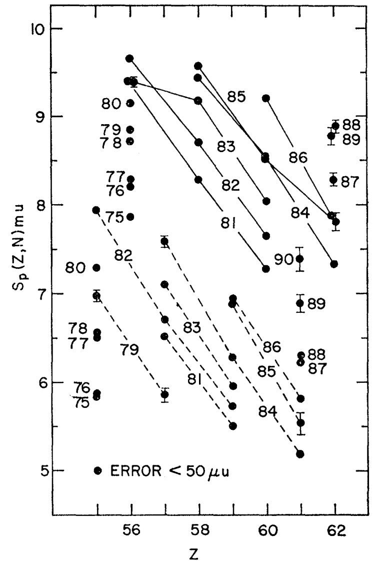

FIG. 8. Proton separation energy as a function of Z.

preferred mixing of states leading to increased stability over the simple filling of 2 nucleons into the $j=\frac{3}{2}$ state with the ensuing reduction of pairing energy. After the shell closure the expected level configuration[23] is $2f^{7/2}(8)$, $1h^{9/2}(10)$, $3p^{3/2}(4)$, $2f^{5/2}(6)$. While the general trend is to higher pairing energy with increasing N, conclusions as to which levels are being filled are impossible to make. The P_n value at 86 neutrons for praseodymium is believed to reflect the previously mentioned error in a Q value rather than any change in nuclear structure.

The proton separation energies, $S_p(Z,N)$, are shown as a function of Z in Fig. 8. The apparent anomalous points of $S_p(56,83)$, $S_p(60,84)$, and $S_p(62,85)$ have already been discussed in terms of apparent errors in the Q values leading to their evaluation. The rest of the separation energies appear to be quite regular, showing increasing value with increasing N and decreasing value with increasing Z. However, the increase in separation energy is not a uniform function of N. The separation energy of the last proton should be expected to increase with the addition of more neutrons to the nucleus because of symmetry energy. The grouping of separation energies at $Z=55$ might be considered as evidence for increased binding for this odd proton in the presence of an odd neutron. A trend of a similar grouping at $Z=56$ might lead one to infer decreased binding of the even proton in the presence of an odd neutron. This grouping trend seems to diminish when the neutron number approaches the closing of the shell at $N=82$. Similar grouping of neutron separation energies may be noted for $N\leqq 79$ wherein the roles of protons and neutrons in the above analysis are reversed. This apparent change in separation energies is probably due to an odd proton-neutron interaction which in this case is more pronounced when the nucleus is not too close to a filled neutron shell. There seems to be no large effect on the proton separation energies caused by the shell closure at 82 neutrons.

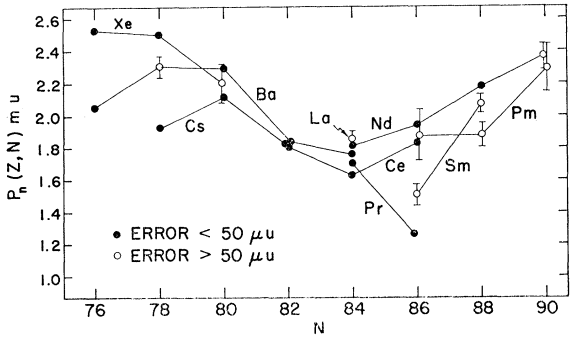

FIG. 7. Neutron pairing energy as a function of N.

The double proton separation energies shown in Fig. 9 appear quite regular, and seem to indicate no large changes in structure in this region, particularly with respect to the neutron shell closure at 82 neutrons.

The proton pairing energies shown in Fig. 10 seem to exhibit no large scale systematic behavior in this region. The expected level configuration of the shell model (Ref. 23, p. 79) in this region is $1g^{7/2}$, $2d^{5/2}$, $1h^{11/2}$. The slight tendency of the pairing energy increase from $Z=56$ to $Z=62$ might be due to the pair formation in the $j=\frac{7}{2}$ level at low Z and in the $j=11/2$ level at high Z. The slight tendency for increased pairing energy for even N may be further evidence for an odd neutron-proton interaction which might slightly disrupt the proton-proton interaction leading to the pairing energy.

From the previous graphs one can determine some general conclusions about nuclear binding energy systematics. The nucleon separation energies calculated from precise mass measurements and accurate nuclear

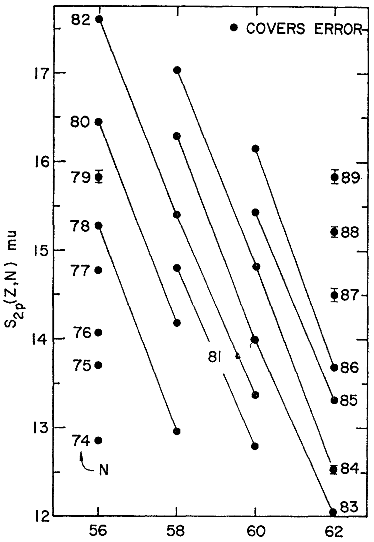

FIG. 9. Separation energy of the last two protons as a function of Z.

reaction and decay Q values seem to be very regular and predictable not only in this present work in the region of $N=82$ but in other mass regions such as covered by Ries *et al.*,[6] Damerow *et al.*,[7] and Barber *et al.*[17] With very few exceptions other than at the magic number shell closures, $S_n(Z,N)$ is an increasing function of Z and a smoothly decreasing function of N, and $S_p(Z,N)$ is an increasing function of N and a smoothly decreasing function of Z. The double nucleon separation energies $S_{2n}(Z,N)$ and $S_{2p}(Z,N)$ are even more smoothly varying functions of N and Z than the single nucleon separation energies. Where data permit calculation of $S_{2n}(Z,N)$ for constant Z and three or four values of N, or $S_{2p}(Z,N)$ for constant N and three or four values of Z, these functions are not only very smooth but in most cases deviate only slightly from linear functions of the variable nucleon number. Even at the magic numbers the abrupt changes in separation energies are very similar as a function of the nonmagic nucleon number.

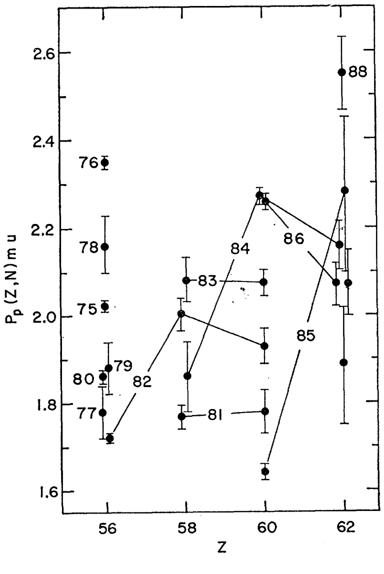

FIG. 10. Proton pairing energy as a function of Z.

This behavior is so uniform that isolated exceptions to it should be considered as strong evidence for errors in data leading to the particular anomalous separation energy. This was the basis used in the previous discussions for rejection or altered assignment of some of the reaction paths used for the calculation of additional atomic masses.

This empirical knowledge of nuclear systematic energies can be used in some cases for the calculation of unknown masses. As an example of this method of calculating an unknown mass, consider the case of La^{137}. Reasonable extrapolations of the separation energy curves give the mass values shown in Table VII.

Note added in proof. We have received pre-publication information from Professor H. E. Duckworth that a number of the measurements, reported originally by Barber *et al.*,[17] have been remeasured. The new results include remeasurement of the neodymium doublets which were discussed earlier in this paper. These new results indicate that the previously reported neodymium mass differences were too large by small but real amounts. Their new results agree well with our neodymium results reported in this paper. These measurements will be reported in a paper by J. D. Macdougall, W. McLatchie, S. Whineray and H. E. Duckworth [Can. J. Phys. (to be published)].

TABLE VII. Mass of La^{137} calculated from extrapolated separation energy curves.[a]

Curve extrapolated	Calculated mass
$S_n(57,N)$	136.906 320±90
$S_{2n}(57,N)$	136.906 380±40
$S_p(Z,58)$	136.906 220±60
$S_p(Z,57)$	136.906 250±60
Average	136.906 310±30

[a] The four separate values are in reasonable agreement with one another and the statistical average with its calculated error of ±30 μu is typical of the precision that may be achieved by this method of mass calculation.

ACKNOWLEDGMENTS

The authors wish to thank Professor A. O. Nier for his continued support and encouragement of this work. We also wish to thank Professor J. H. E. Mattauch for sending to us a copy of the 1964 Atomic Mass Table before publication. We wish to acknowledge the aid of Victor Arnold in maintenance and operation of the instrument. We are also indebted to R. B. Thorness for his aid in design and construction of the spectrometer and to Robert Howard for his aid in design and construction of the electronic circuitry.